ImmunoTargets and Therapy

Dovepress
Taylor & Francis Group

Open Access Full Text Article

ORIGINAL RESEARCH

Development of a Novel Anti-Siglec-15 Antibody for Tumor Immunotherapy

Qin Liu[1,*], Lin Li[1,*], Siji Nian[1], Xiaoke Sun[2], Xiyuan Guo[1], Chengwen Li[1], Zhihui Yang[3], Yingchun Ye[1], Qing Yuan[1,4]

[1]Public Center of Experimental Technology, The School of Basic Medical Sciences, Southwest Medical University, Luzhou, Sichuan, People's Republic of China; [2]Key Laboratory of Medical Electrophysiology of the Ministry of Education, Southwest Medical University, Luzhou, Sichuan, People's Republic of China; [3]Department of Pathology, The Affiliated Hospital of Southwest Medical University, Luzhou, Sichuan, People's Republic of China; [4]Institute of Nuclear Medicine, Southwest Medical University, Luzhou, Sichuan, People's Republic of China

*These authors contributed equally to this work

Correspondence: Qing Yuan; Yingchun Ye, Southwest Medical University, No. 1, Xianglin Road, Luzhou, Sichuan, 646000, People's Republic of China, Email qingyuan@swmu.edu.cn; yeyingchun@swmu.edu.cn

Purpose: As a novel candidate in cancer immunotherapy, siglec-15-targeting antibodies hold promise for providing alternative therapeutic strategies to tumors unresponsive to programmed death ligand 1 (PD-L1) antibody therapy. To date, pharmacological development targeting siglec-15 has not yet achieved significant breakthroughs or clinical approval. Therefore, this study aims to develop a novel anti-siglec-15 antibody designed to restore tumor immune normalization.

Methods: In this study, we constructed a phage immune library derived from lymphoid tissues of lung cancer patients using phage display technology and screened the fully human antibodies against siglec-15 antigen from this library. The antibody affinity was detected by Bio-Layer Interferometry, the binding rate of antibody to positively expressing siglec-15 tumor cells was examined by flow cytometry, and the activity of antibody-mediated killer cells against tumor cells was reflected by Antibody-Dependent Cellular Cytotoxicity (ADCC) action. The blockage of proliferation inhibition caused by siglec-15 antigen by antibodies was investigated by t-lymphocyte proliferation assays, and $CD8^+$ T cells were collected from malignant pleural effusion specimens derived from lung cancer patients to determinewhether antibodies could alleviate the immunosuppression present in the tumor microenvironment (TME). The anti-tumor efficacy of the antibody was investigated in vivo by constructing a zebrafish tumor model and a humanized mouse tumor model.

Results: The antibody demonstrated nanomolar affinity and specificity, enhanced antibody-dependent cellular cytotoxicity (ADCC) against tumor cells, reversed T-cell suppression, and reduced $CD8^+$ T-cell exhaustion in vitro analyses. In vivo models confirmed tumor growth inhibition via increased lymphocyte infiltration and activation.

Conclusion: Antibody immune libraries from lymphoid tissues of lung cancer patients can screen specific antibodies against siglec-15 target antigens and exert certain biological functions in vitro and in vivo.

Plain Language Summary: Following PD-1/PD-L1 blockade, siglec-15 has emerged as a compelling therapeutic target for tumor immune normalization, with its specific antibodies potentially addressing clinical resistance to PD-1 inhibitors. Utilizing phage display technology, we developed a lung cancer patient-derived immune library and isolated a novel anti-siglec-15 antibody exhibiting nanomolar affinity and precise antigen specificity, as rigorously validated through Bio-Layer Interferometry (BLI) and ELISA. Functional characterization demonstrated the antibody's dual mechanism: enhancing lymphocyte-mediated ADCC against tumor cells while reversing siglec-15-induced suppression of T-cell proliferation. Notably, in vitro analyses of malignant pleural effusions, the antibody significantly reduced $CD8^+$ T-cell exhaustion. We found that anti-siglec-15 recombinant antibodies inhibited tumor growth by increasing lymphocyte infiltration and activation in tumor tissues by constructing a zebrafish tumor model and a PBMC humanized mouse tumor model. These findings provide a theoretical framework for the development of anti-siglec-15 targeting antibody drugs and tumor immunonormalization therapy.

Keywords: phage display technology, lymphocyte infiltration, T-cell suppression, malignant pleural effusion, tumor microenvironment

Received: 26 May 2025
Accepted: 19 November 2025
Published: 11 December 2025

Graphical Abstract

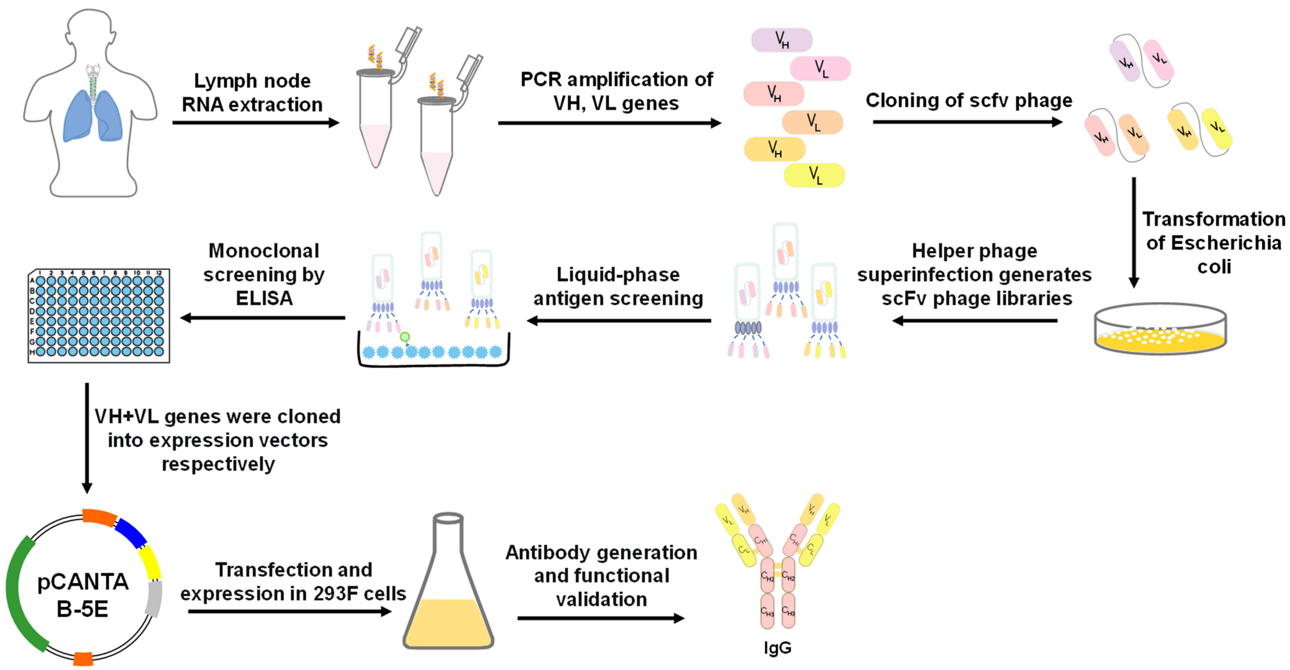

Introduction

In the past decade, through clinical research and observation, researchers have identified an important phenomenon - systemic immune activation does not necessarily lead to cancer regression, especially in the treatment of patients with solid tumors.[1] Passive enhancement of immunity is usually associated with adverse immune reactions.[2–4] Therefore, cancer immunotherapeutic strategies need to shift from traditional immune enhancement therapies to targeting the tumor microenvironment based on tumor-induced immune escape mechanisms for the development of more effective and less toxic immune normalization therapeutic strategies.[5]

By administering PD-1 therapy, researchers have highlighted the importance of restoring the immune suppression in the tumor microenvironment (TME) as a principle for normalizing cancer immunotherapy. Immune dysfunction caused by the B7-H1/PD-1 pathway occurs in less than 40% of human solid tumors, based on the recent definition of the immune classification of tumors in the TME.[6–8] Several studies have suggested that in addition to the upregulation of B7-H1, many other molecular and cellular mechanisms can contribute to immune dysfunction in TME.[9,10] Siglec-15 is a new player in the field of cancer immunotherapy, which may act as a novel class of immunosuppressants. Its expression is associated with tumors, and its mechanism of action differs from that of PD-L1. Thus, it might be used as a new therapeutic tool for treating anti-PD-1/PD-L1-resistant patients.

Siglec-15, an emerging oncogenic target with PD-L1 homology, modulates tumor microenvironment via SYK/MAPK signaling in tumor-associated macrophages.[11] Siglec15 significantly inhibits antigen-specific T cell responses in vivo and in vitro, and suppresses immune responses and triggers immune escape in tumor microenvironments.[12] This demonstrates that siglec-15 serves as an important immunosuppressive molecule in the tumor microenvironment. Siglec15 is poorly expressed in most normal tissues and immune cell subsets, and is significantly expressed by M2-type macrophages in the tumor microenvironment, as well as in tumors including lung, ovarian, head and neck, intestinal, thyroid, bladder, kidney, and liver cancers.[13,14] David Rimm et al found that siglec15 expression was relatively higher in EGFR mutant lung cancers.[15] In a study of bladder cancer (BLCA), Hu et al demonstrated that siglec15 expression was mutually exclusive with several immune checkpoints in BLCA, including PD-L1, PD-1, CTLA-4, and LAG-3, and that the overexpression

 https://doi.org/10.2147/ITT.S536009

pattern of siglec15 was TME-specific.[16] These findings indicate that siglec-15 is highly expressed in multiple types of solid tumors and correlated with poor prognosis. NC318, developed by NextCure as the leading candidate, was the only Siglec-15 monoclonal antibody to reach clinical trials. However, its development was terminated in November 2022. Preclinical research on Siglec-15 antibodies continues, with a novel monoclonal antibody, PYX-106, currently under evaluation in PYX-106-101 - a first-in-human, open-label, non-randomized, Phase 1 dose-escalation study in patients with advanced cancer.[17] To date, no significant breakthroughs have been reported in siglec-15 drug development, and no therapeutics targeting this pathway have reached the market. Thus, siglec-15 remains a promising target meriting further in-depth exploration.

In this study, we constructed a fully human phage immune library with a large capacity, identified high-affinity antibodies targeting siglec-15, and investigated their antitumor biological functions. We aimed to develop a new immunotherapeutic tool for targeting malignant tumors.

Materials and Methods

Tissues and Body Fluids

After obtaining informed consent from patients and their families, postoperative tumor tissues, lymphoid tissues, and pleural effusions were collected from lung cancer patients in the Department of Thoracic Surgery at the Affiliated Hospital of Southwest Medical University. This study complied with the provisions of the Declaration of Helsinki. Ethical approval was obtained for all research involving human or animal subjects, and informed consent was obtained from all human participants. Approval for human research was granted by the Experimental Ethics Committee of the Affiliated Hospital of Southwest Medical University (KY2023277), and for animal research by the Animal Experiment Ethics Committee of Southwest Medical University (20220812–030).

Cell Lines

PC-3, HepG2, A549, MCF-7, 16HBE, HEK293F, and HEK293T were obtained from the American Type Culture Collection (ATCC), while Talent Biotechnology Corporation provided T24 and NCI-H157. Cells such as MCF-7, 16HBE, T24, HepG2, and HEK293T were cultivated in DMEM (Gibco, USA) media supplemented with 10% FBS (NEWZERUM, New Zealand). PC-3, A549, and NCI-H157 cells were grown in RPMI 1640 (Gibco, USA) media with 10% FBS. SMM293-T1 (SinoBiological, CA) media was used to cultivate HEK293F. The aforementioned cells were kept in an incubator (Thermo, USA) with a controlled temperature and humidity at 37°C and 5% CO_2. At the time of the experiment, every cell had been cultivated for more than three generations and was in the logarithmic growth phase.

Library Construction and Anti-siglec15 Single-Chain Antibody Screening

Lymph Node RNA Extraction from Lung Cancer Patients and Construction of a Fully Human scFv Phage Library

The library construction protocol was performed according to our previous report.[18] TRIzol reagent (Invitrogen, USA) was used to extract total RNA from the lymph nodes of over thirty lung cancer patients. cDNA reverse transcription was then carried out. The heavy chain variable structural domain (VH) and light chain variable structural domain (VL, including Vλ and Vκ) of antibody fragments were amplified using PCR. Following purification, the VH and VL DNAs from various patients were combined, and the purified VH and VL were utilized as templates for overlapping PCR amplification to produce the VH-Vκ and VH-Vλ genes. The downstream primers and upstream primers for amplification of VH and VL were designed as described in the references.[18,19] In order to evaluate the diversity of the scFv libraries, the VH-Vκ and VH-Vλ genes were proportionately mixed, restriction endonuclease digested, and ligated with the phage vector pCANTAB-5E. The bacterial fluids were then collected and preserved, and randomly chosen single colonies of the libraries were identified by PCR.[20]

Phage Enrichment and Screening of Human Anti-Siglec-15 Antibody

The following experiments were performed as described in our previous study.[18] First, liquid phase screening was performed, in which biotinylated siglec-15 antigen first interacted with the scFv library in a liquid reaction system. Then, Dynabeads M-280 (Invitrogen, USA) was added to enrich for scFvs that could bind to the human siglec-15 antigen (Novoprotein, CA). Enrichment and screening of siglec-15-scFv libraries were conducted in three rounds, after which 20 monoclonal colonies were randomly selected for siglec-15-scFv library diversity identification. Next, 48 monoclonal colonies were randomly selected for amplifying the scFv phage. Siglec-15 antigen (diluted to 3 μg/mL) was used for plate-coating, and the monoclonal antibody Anti-M13 Antibody (HRP) (SinoBiological, CA) was used as the secondary antibody at 1:5000 dilution. Finally, tetramethylbenzidine (TMB) (Invitrogen, USA) was added to color development. Positive clones were identified by the OD values; specifically, their OD values were 2.5-fold greater than the OD values of negative controls. After sequencing, correctly sequenced siglec-15-scFv was used as a candidate clone.

Anti-siglec15 IgG1 Antibody Construction and Binding Activity Detection

Anti-siglec15 IgG1 Antibody Expression, Purification, and Characterization

The VH and VL of siglec-15-scFv gene were cloned into the constructed expression plasmids encoding human IgG1 CH and Cλ sequences, CH-pcDNA3.4 and Cλ-pcDNA3.4, using the SE Seamless Cloning and Assembly Kit (Zomanbio, CA). The recombinant plasmids were extracted and transfected into FreeStyle™ 293-F cells. After 7 days of transient transfection, the cell supernatant was collected and purified with protein A affinity chromatography column (GE, USA).

Identification of Anti-Siglec-15 Antibody Binding Activity and Cross-Reactivity by ELISA

After being diluted to 1 μg/mL, human EphA2 (hEphA2), hTrop2, hCD24, hsiglec-15, and hB7-H3 (Novoprotein, USA) were plate-coated at 4°C for an overnight duration. The binding activity of the anti-siglec-15 antibody to the siglec-15 antigen and cross-reactivity with other highly expressed proteins in cancer were detected by ELISA analysis, as previously reported.[21]

Identification of Anti-Siglec-15 Antibody Affinity by Bio-Layer Interferometry

Using Bio-Layer Interferometry (BLI), the recombinant antibody's binding affinity to the siglec-15 protein was investigated. BLI studies were carried out according to earlier descriptions.[18] After being diluted in 1× PBST, biotinylated siglec-15 protein was connected to the SA biosensor (Pall ForteBio, Fremont, CA). Next, 200 μL of purified IgG1 antibody against siglec-15 (5 μg/mL, 10 μg/mL, and 20 μg/mL) was used to assess antigen-antibody interactions. Antigen-antibody binding and dissociation were systematically analyzed to get equilibrium dissociation constant (KD) values. The Data Acquisition 9.0 software was used to evaluate the collected data.

Detection of Antibody-Binding Activity by Flow Cytometry

First, we established a stable cell line that overexpress siglec-15. After transfecting HEK293T cells with the commercial lentiviral vector plasmid pSLenti-EF1-EGFP-P2A-PurO-CMV-MCS-3XFLAG-WPRE (Obiosh, CA), the supernatant was collected and infected with A549 cells at 48 h. After 72 h, the cells were visualized for fluorescence under a fluorescence microscope and screened for pressurization using puromycin to establish the stably transfected cell line S15-A549.

Binding of anti-siglec-15 antibody to tumor cells (including A549 overexpressing siglec 15) was detected by flow cytometry. Tumor cells were prepared (1×105 cells/test), and then, different concentrations of S131-IgG1 were added (starting at 20 μg/mL, two-fold concentration gradient dilutions). After incubating the cells at 4°C for 1 h, Rabbit Anti-Human IgG H&L/Alexa Fluor 647 antibodies (Bioss, CA) were added at 1:500 dilution, and incubated again at 4°C for 1 h. After incubation, the cells were washed and fluorescence was detected by flow cytometry (ACEA). All experiments were performed in triplicate, with each experimental group containing a minimum of three replicates. The results were analyzed using the FlowJo 10.2 software.

Detection of Anti-Siglec-15 Antibody Binding Activity by Cellular Immunofluorescence

First, 1×10^5 cells were placed on polylysine coverslips and incubated for 24 h. The cells were washed with 1×PBS and fixed with 4% paraformaldehyde for 10 min at room temperature, and then blocked for 30 min at room temperature in blocking buffer (1×PBST containing 10% goat serum). Next, 20 μg/mL S131-IgG1 was added, and the cells were incubated overnight at 4°C. After washing, Goat Anti-Human IgG H&L/AF594 antibody (Bioss, CA) 1:200 was added

https://doi.org/10.2147/ITT.S536009

and incubated in the dark for 1 h. Antifade Mounting Medium with DAPI (Beyotime, CA) was added to the samples, the coverslips were covered, and images were captured under a fluorescence microscope.

Identification of Anti-Tumor Activity of Anti-siglec15 IgG1 Antibody

ADCC Activity

PBMC were isolated as effector cells from healthy human peripheral blood using the FICOLL PAQUE PREMIUM (Cytiva, USA), and A549, PC-3 and S15-A549 were used as target cells. PBMC and target cells were co-cultured with or without anti-siglec15 IgG1 antibody. Cytotoxicity was identified using the CytoTox 96® Non-Radioactive Cytotoxicity Assay (Promega, USA). All experiments were performed in triplicate, with each experimental group containing a minimum of three replicates.

Lymphocyte Proliferation

Anti-human CD3 (Biolegend, USA) was added to 96-well plates at a final concentration of 0.5 μg/mL and incubated at 4°C overnight. PBMCs (3×10^6 cells/mL) from healthy volunteers, labeled with 5 μM CFSE (Biolegend, USA), was added to each well. Additionally, 5 μg/mL human siglec-15 protein was added to each well, with or without the siglec-15 antibody (20 μg/mL), The cells were cultured for 72 h and collected for flow cytometry analysis. To determine whether T cell subsets underwent proliferation, FITC anti-Human CD3 Antibody (Biolegend, USA), APC/Cyanine7 anti-Human CD8 Antibody (Biolegend, USA), and APC anti-human CD4 Antibody (Biolegend, USA) were incubated at 4°C for 30 min for staining the surface of cells. After washing, 7-AAD (BD, USA) was used to exclude dead cells, and the labeled cells were analyzed by flow cytometry. All experiments were performed in triplicate, with each experimental group containing a minimum of three replicates.

Detection of T Lymphocyte Apoptosis and Activity

Ultra-LEAF™ Purified anti-human CD3 antibody (Biolegend, USA) was coated onto 96-well plates at a final concentration of 0.5 μg/mL (100 μL/well) and incubated overnight at 4°C. Malignant pleural effusions from lung cancer patients ($n \geq 6$) were collected, and lymphocytes were isolated using Ficoll-Paque™ PREMIUM density gradient medium (Cytiva, USA). The cell density was adjusted to 3×10^6 cells/mL, and 100 μL was added to each well. Ultra-LEAF™ Purified anti-human CD28 antibody (Biolegend, USA) was then supplemented to each well at a final concentration of 0.5 μg/mL. Cells were cultured for 72 hours with or without S131-IgG1/S194-IgG1/Nivolumab (20 μg/mL) and subsequently harvested for flow cytometry analysis. Apoptosis was detected using the FITC Annexin V Apoptosis Detection Kit I (BD, USA). To evaluate the functional restoration of T cells in vitro, PE-Cy7 anti-human IFN-γ antibody (BD, USA) and PE anti-human Granzyme B antibody (BD, USA) were applied.

Zebrafish Tumor Model

Wild-type AB zebrafish were obtained from the Zebrafish Technology Platform of Southwest Medical University. The rearing conditions were strictly controlled at 28°C, pH (6.5–8.5). Male and female zebrafish were mixed in a ratio of 2:2 to prevent predation of eggs after obtaining embryos. Abnormal embryos were removed. The age of the embryos was expressed in hours (hpf) or days (dpf) after fertilization. Zebrafish at 48 hpf were used in this experiment without sex preference. PBMC were fluorescently labeled with Dio (Beyotime, USA) according to the manufacturer's instructions after three days of stimulation with anti-human CD3 andanti-human CD28 (Biolegend, USA). The cell line A549 was labeled with Dil (Servicebio, USA). After the embryos were cultured to 48 hpf and manually stripped of membranes, approximately 200–400 cells were injected into each zebrafish yolk sac using a microinjector after mixing fluorescently labeled A549 cells and PBMC cells in a 9:1 ratio. We chose zebrafish with sufficient fluorescence of tumor cells and randomly divided them into groups of at least 5 fish each. PBS was used as a negative control group and S131-IgG1 was used as a treatment group. 1 nl was injected intravenously every day, and the growth and migration of tumor cells were monitored three days after treatment (dpi) using a somatic fluorescence microscope (Olympus Imaging). The zebrafish study was approved by the Animal Ethics Committee of Southwest Medical University.

Mouse Tumor Model

This study complied with the provisions of the Declaration of Helsinki. All mouse experiments were approved by the Animal Ethics Committee of Southwest Medical University (NO.20211122–050) and carried out in conformity with the Guide for the Care and Use of Laboratory Animals. Female NTG mice (6–8 weeks old) were purchased from Beijing SiPeiFu Biotechnology Corporation and housed in the SPF (Specific Pathogen-Free) environment of the Experimental Animal Center of Southwest Medical University. The use and treatment of mice strictly followed the guidelines for the care and use of research animals, and all experiments were approved by the Animal Ethics Committee of Southwest Medical University. Each mouse was subcutaneously inoculated with A549 cells at a density of 3×10^6. When the tumor volume reached about 80 mm^3, the mice were injected with 1×10^7 PBMCs collected from healthy volunteers through the tail vein. One week after the injection, the mice were randomly divided into two groups (n = 6 mice/group). PBS was administered to the mice in the negative control group, and S131-IgG1 was administered to those in the treatment group. The antibody was administered intravenously via tail vein at 15 mg/kg body weight every three days for two weeks. Tumor volume and body weight were monitored throughout the treatment period. The tumor volume was calculated by the formula: Tumor volume (mm^3) = $1/2\times$length$\times$width^2. At the end of the treatment period, all mice were euthanized. Peripheral blood was collected for isolating peripheral blood mononuclear cells (PBMCs) for flow cytometry analysis. Tumor tissues were processed into single-cell suspensions for flow cytometry analysis. Cells were stained with anti-human CD45-PE, anti-mouse CD45-PE-Cy7, anti-human CD3-FITC, anti-human CD4-APC, anti-human CD8-APC-Cy7, and LIVE/DEAD™ 7-AAD. Following dead cell exclusion, successful immune system humanization was confirmed by detection of ≥25% human CD45+ T cells. Tumor tissues were dissociated into single-cell suspensions using the Miltenyi Biotec Tumor Dissociation Kit on the gentleMACS™ Dissociator with Heater. Subsequent staining utilized LIVE/DEAD™ Zombie Red™, anti-human CD45-PE, anti-human CD3-FITC, anti-human CD4-APC, anti-human CD8-APC-Cy7, anti-human CD69-BV785, anti-human GZMB-BV421, and anti-human IFN-γ-PE-Cy7 to evaluate T cell activation and cytotoxic function.

Statistical Analysis

The statistical analysis was carried out utilizing GraphPad Prism 9.0. The data were presented as mean (±SD) or mean ± standard deviation. The *t*-test was used to determine significance in order to compare the two groups. P>0.05 was considered not statistically significant (ns), *P<0.05, **P<0.01, ***P<0.001.

Results

A Fully Human scFv Phage Immunizing Antibody Library Was Constructed with a Large Library Capacity and Good Diversity

The first-strand cDNA was synthesized from the mRNA extracted from lymph node tissues of 20 lung cancer patients. Using the synthesized cDNA as a template, the size of the amplified VH, Vλ, and Vκ gene bands was found to be about 400 bp (Figure S1A–C). The VH-linker-VL gene library (about 800 bp) was obtained by two rounds of overlapping extension PCR (SOE-PCR) (Figure S1D), and a fully human scFv phage display library was constructed. The DNA in the scFv library was ligated with the phage vector pCANTAB-5E and transformed into *E. coli* TG1. Next, 21 monoclonal colonies were randomly selected, and PCR was performed to identify the scFv insert fragments (Figure S1E). The results showed that all monoclonal colonies were inserted with full-length scFvs genes, and 15 colony DNAs were selected for BstNI digestion. The DNA fingerprinting results showed that each scFv was different (Figure S1F), the constructed phage library of human scFvs was diversified, and the gene sequences in the antibody libraries were enriched.

Fully Human IgG1 Antibodies with High Specificity and Affinity Were Screened and Constructed

Affinity Screening of Siglec-15-scFv

After three rounds of enrichment screening, the size of the input libraries decreased, while the size of the output libraries increased after enrichment. These changes greatly enriched the antibody clones against the target antigen (Figure 1A and B).

A

Screening round	Input	Output	Input/ Output
1st round	1.3×10^{11}	7×10^{4}	1.85×10^{6}
2nd round	7×10^{10}	2.9×10^{5}	2.4×10^{5}
3rd round	3×10^{10}	3.04×10^{6}	1.2×10^{4}

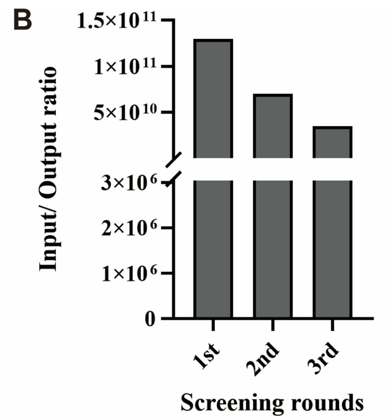

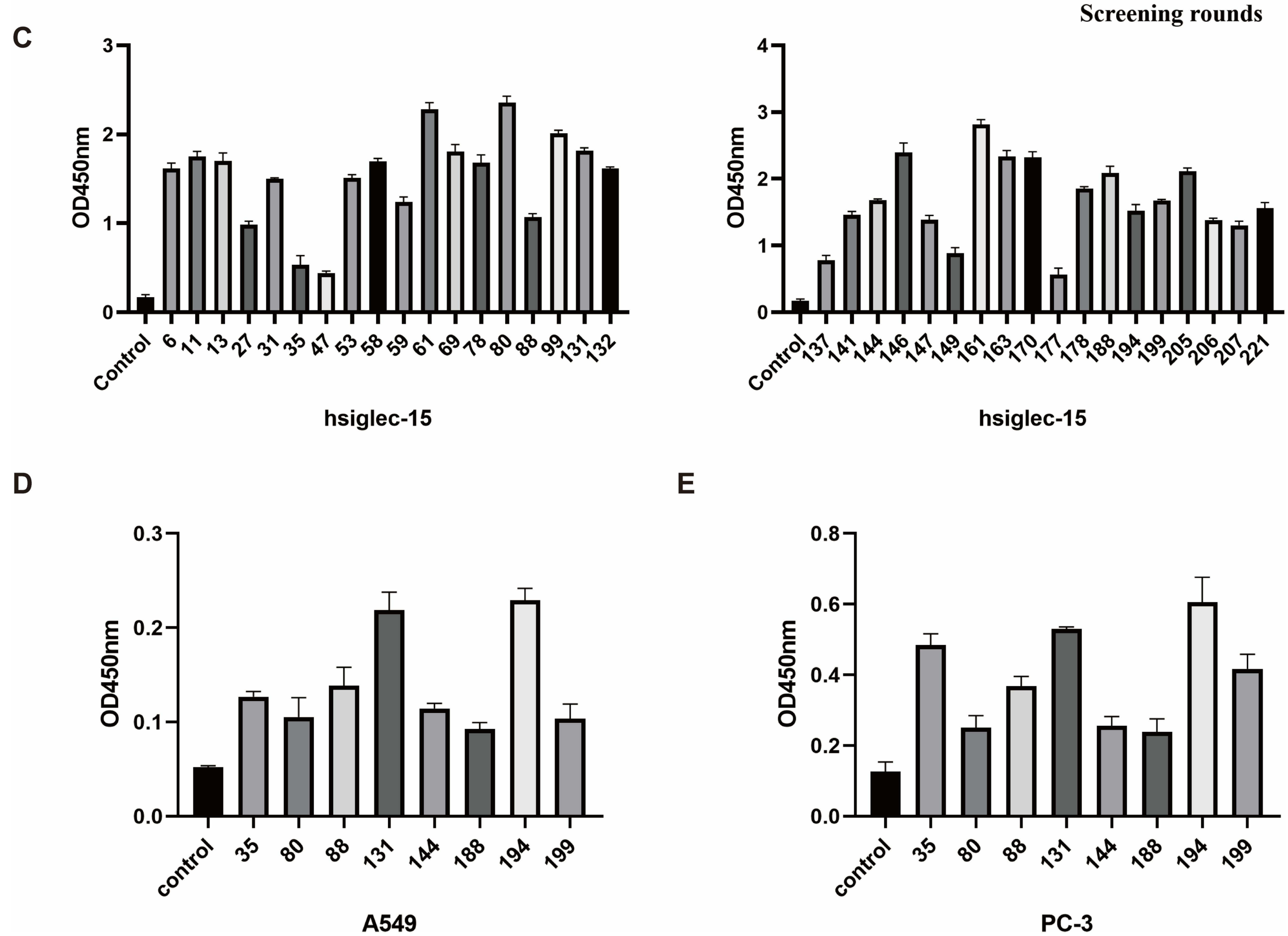

Figure 1 High-Affinity scFv Screening. (**A** and **B)** The phage antibody libraries were screened against the siglec-15 antigen, and their input, output, and input-to-output ratios were determined. (**C**) ELISA was performed to characterize the binding activity of 36 scFvs, which was initially screened against the target antigen siglec-15. (**D**) ELISA was performed to characterize the binding of the 8 screened scFvs to A549 cells. (**E**) ELISA was performed to identify the binding of the 8 screened scFvs to PC-3 cells.

After three rounds of enrichment affinity screening, 230 monoclonal colonies were randomly selected for expression, and the binding activity of siglec-15 scFv was evaluated by ELISA. In total, 51 positive strains were screened based on the results obtained at OD450. The positive strains were analyzed by ELISA again to test whether the strains stably expressed scFvs and identify scFvs that could bind strongly to the target antigen siglec-15. The results showed that 36 scfvs were ELISA positive (Figure 1C). The OD values of positive responses were twice as high as those of the negative values. The binding activity of the screened scFvs to tumor cells (PC-3 and A549) was assessed, and eight positive scFvs were finally screened (Figure 1D and E), which were sequenced for subsequent experiments.

 https://doi.org/10.2147/ITT.S536009

Anti-siglec15 IgG1 Antibody Expression, Purification, and Characterization

Based on the results of multiple ELISA and DNA sequencing, 2 scFvs with different gene sequences and high affinity were screened to construct recombinant antibodies. Whether siglec-15-IgG1 was successfully constructed was verified by DNA sequencing. The constructed expression plasmids were transiently co-transfected with HEK 293F eukaryotic cells; the cell supernatants were collected and purified on day 7. According to the 250 kDa protein ladder marker, both siglec-15 antibodies exhibit a heavy chain size of approximately 50 kDa, whereas the light chain of S131-IgG1 is approximately 30 kDa and that of S194-IgG1 is approximately 25 kDa (Figure 2A). The marker exhibited clear gradient resolution, with no evident non-specific bands or high-molecular-weight smearing observed, indicating high antibody purity and minimal degradation.

BLI and ELISA Showed That the Recombinant Antibody Had Good Antigen-Binding Activity and Specificity

The antigen-antibody affinities of positive scFvs of different sequences were examined using the macromolecular interaction technique. Both S131-IgG1 and S194-IgG1 had higher affinities (Figure 2B and C), which reached nanomolar (10^{-9}) and picomolar (10^{-12}) levels, respectively. The results of ELISA showed that S131-IgG1 and S194-IgG1 recognized siglec-15 antigens in a dosage-dependent manner (Figure 2D), but they did not bind to four antigens, EphA2, B7-H3, Trop2 and CD24), which were expressed at high levels on tumor (Figure 2E and F). The high affinity and specificity of the recombinant antibody acted as a suitable candidate for the subsequent validation of the antitumor function.

Flow Cytometry and Immunofluorescence Were Performed to Detect the Binding of Recombinant Antibodies to Tumor Cell Surface Antigens

The binding affinity of the recombinant antibody siglec-15-IgG1 to soluble siglec-15 antigens was determined using the macromolecular interaction technique. After screening S131-IgG1 and S194-IgG1 antibodies with high affinity, flow cytometry assays were performed to detect the binding activity of the two recombinant antibodies to the normal epithelial cell line 16-HBE, and tumor cell lines T24, PC-3, NCI-H157, A549. In addition, we overexpressed siglec-15 in the A549 cell line, by constructing the A549 cell line that could stably express siglec-15 protein. The results showed that S131-IgG1 had relatively high binding efficiency and stronger binding affinity to lung adenocarcinoma cell lines A549 and NCI-H157. Moreover, the binding ability of the antibodies further increased with an increase in the expression of the siglec-15 protein by tumor cells (Figure 3A). The cellular immunofluorescence results also showed that the recombinant antibodies could bind to tumor cells with positive siglec-15 expression (Figure 3B).

Anti-siglec15 IgG1 Antibody Showed Good Anti-Tumor Effects at the Cellular Level

Antibody-Dependent Cytotoxic Effects and Inhibition of Tumor Cell Proliferation

To evaluate the cytotoxic effects of the full-length antibodies S131-IgG1 and S194-IgG1 on the siglec-15-overexpressing A549 cell line (S15-A549), we used the CCK8 method to determine the inhibitory effects of different concentrations of antibodies on tumor cells. The results showed that S131-IgG1 and S194-IgG1 did not directly inhibit the S15-A549 tumor cells (Figure 4A). By assessing the ADCC effect exerted by the full-length antibodies S131-IgG1 and S194-IgG1, we found that these antibodies mediated the killing activity of human PBMCs against S15-A549 tumor cells when the ratio between effector cells and target cells was 10:1 for PC-3, A549, and S15-A549 cells. The strongest cytotoxic effect was mediated against S15-A549 cells (Figure 4B). This finding suggested that recombinant antibodies act mainly through antibody-mediated cytotoxicity without significantly affecting the proliferation of tumor cells.

Recombinant Antibodies Partly Relieved the Inhibition of T-Lymphocyte Proliferation by the Siglec-15 Antigen

Proliferation of T cells was detected using anti-CD3 antibody-activated human PBMC cells with the addition of hsiglec15 protein with or without anti-siglec15 antibodies The results showed that the proliferation of $CD3^{+}$T, $CD4^{+}$T, and $CD8^{+}$T cells was inhibited in the siglec-15 antigen group compared to their proliferation in the normal lymphocyte control group (Figure 4C). This finding indicated that siglec15 partly inhibited lymphocyte proliferation. When S131-IgG1/S194-IgG1 was added, the proliferation of $CD3^{+}$T, $CD4^{+}$T and $CD8^{+}$T cells was significantly enhanced compared with the antigen group, and was similar to that of the normal proliferation group (Figure 4C). These results suggested that the recombinant antibodies could relieve the inhibition of the proliferation of human lymphocytes mediated by siglec-15, and could partially restore the function of T cells.

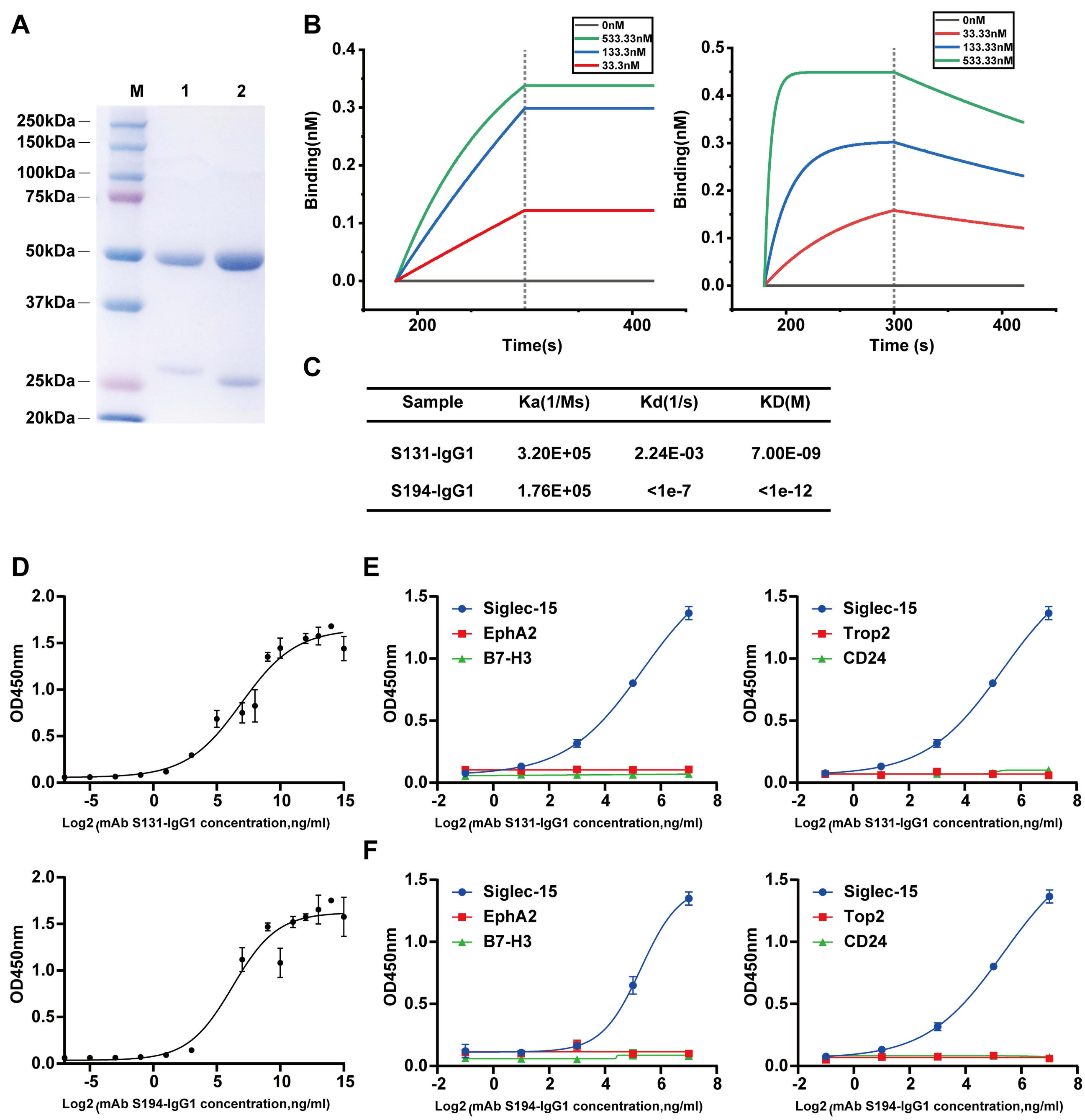

Figure 2 Purification, Characterization, and Antigen-Binding Analysis of Recombinant Antibodies. (**A**) SDS-PAGE was performed to identify purified recombinant antibody siglec15-IgG1; 1 indicates S131-IgG1 and 2 indicates S194-IgG1. (**B**) The binding and dissociation curves of S194-IgG1 and S131-IgG1 with biotin-labeled Siglec-15 protein were shown. (**C**) Macromolecular interaction data of S194-IgG1 and S131-IgG1 bound to biotin-labeled Siglec-15 proteins were presented; Ka represents the association constant, Kd represents the dissociation constant, and KD represents the equilibrium dissociation constant. (**D**) The binding reaction curves of recombinant antibodies S131-IgG1 and S194-IgG1 with siglec-15 protein are shown. (**E**) The binding reaction curves of the recombinant antibody S131-IgG1 to EphA2, B7-H3, Trop2, and CD24 proteins are shown. (**F**) The binding reaction curves of the recombinant antibody S194-IgG1 to EphA2, B7-H3, Trop2, and CD24 proteins are shown.

The Recombinant Antibodies Decreased the Apoptosis of Exhausted CD8+ T Cells and Promoted the Production of Granzyme B

Flow cytometry was employed to assess the in vitro restoration of T cell function by S131-IgG1 or S194-IgG1 in T cells isolated from malignant pleural effusions of lung cancer patients (Figure 5A and B). The results of apoptosis showed that S131-IgG1 and S194-IgG1 decreased the apoptosis of T cells compared with the untreated group (control) and S131-IgG1 was significantly more effective in reversing T-cell apoptosis (Figure 5C). In addition, S131-IgG1 and S194-IgG1

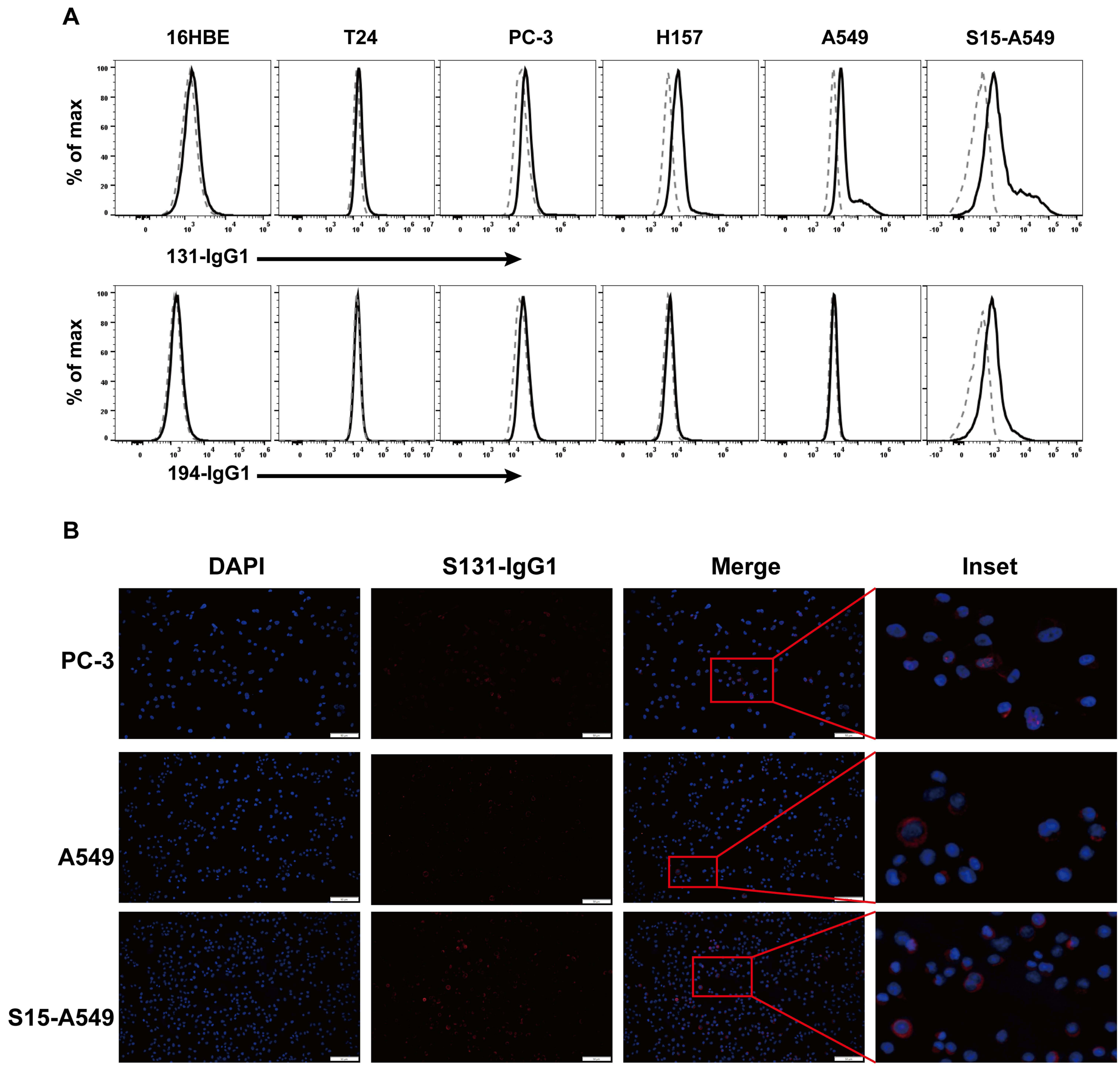

Figure 3 Antibody Binding to Tumor Cells. (**A**) Flow cytometry assays were performed to evaluate recombinant antibody binding to the normal epithelial cell line 16-HBE, tumor cell lines T24, PC-3, NCI-H157, A549, and an A549 tumor cell line overexpressing siglec −15 (S15-A549); the gray dashed line denotes the control group, and the black solid line denotes the experimental group. (**B**) immunofluorescence detection of the binding of the recombinant antibody S131-IgG1 to PC-3, A549, and S15-A549 cells was performed, The magnified inset reveals detailed features of tumor cells (from the boxed region in the main figure), clearly demonstrating S131-IgG1 binding to Siglec-15 protein (red).

promoted the secretion of GZMB by CD8+T cells, but they had no significant effect on IFN-γ secretion by CD8+T cells (Figure 5D and E). The results of in vitro experiments showed that the siglec-15 recombinant antibody decreased the apoptosis of $CD8^+$ T cells and promoted the production of GZMB by $CD8^+$ T cells. Next, the S131-IgG1 antibody with better in vitro function will be used for in vivo anti-tumor studies.

Anti-Siglec15 IgG1 Antibody Showed Promising Anti-Tumor Effects in Animal Tumor Models

Anti-siglec15 IgG1 Antibody Inhibited Tumor Growth in a Zebrafish Tumor Model

We administered S131-IgG1 intravenously to zebrafish inoculated with Dil-A549 and Dio-PBMC cells and evaluated the anti-tumor effect of S131-IgG1 by the changes in fluorescence intensity (Figure 6A). Compared with the control group,

 https://doi.org/10.2147/ITT.S536009

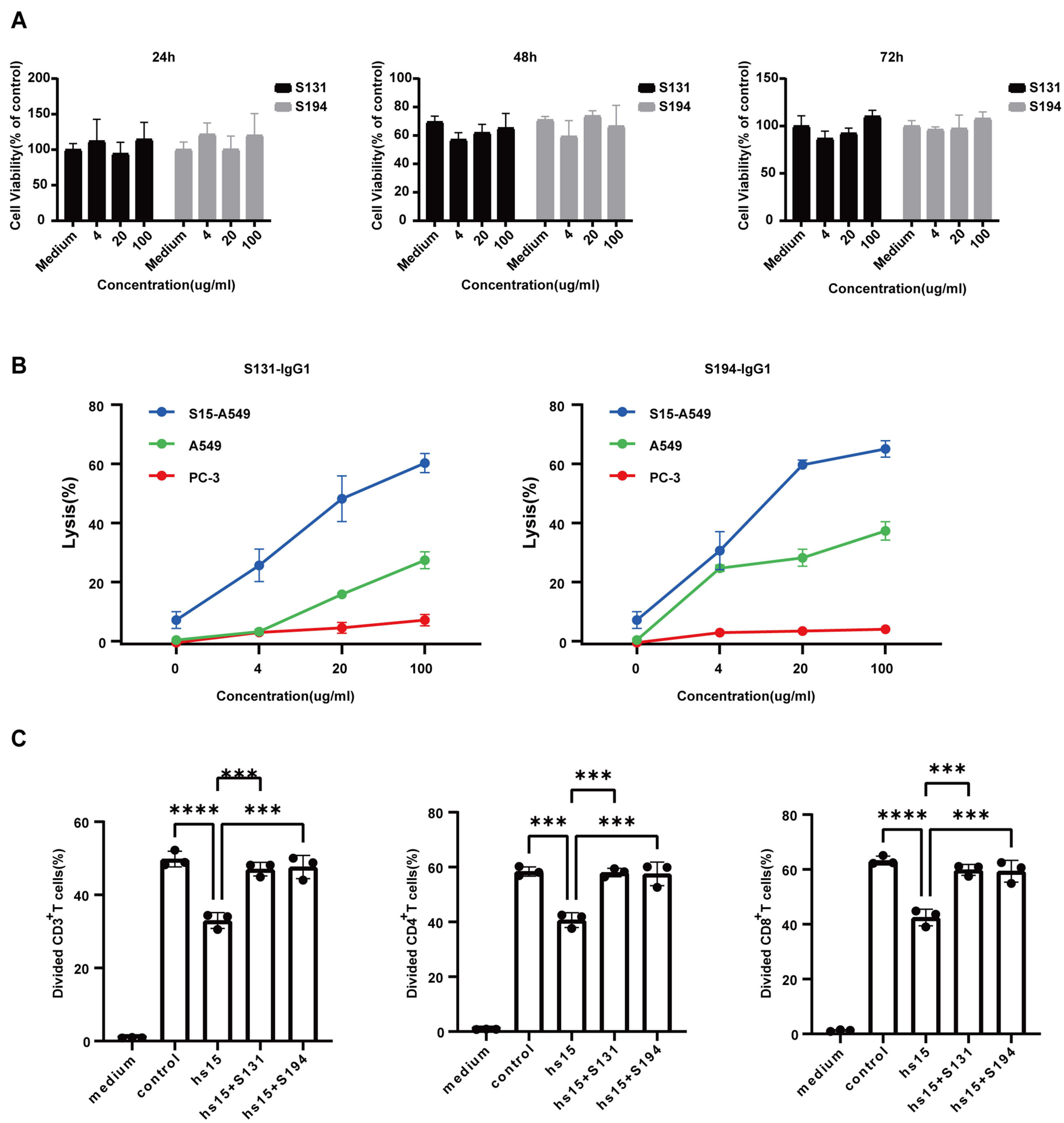

Figure 4 Antitumor Activity at the Cellular Level. (**A**) The inhibition of the proliferation of S15-A549 tumor cells by S131-IgG1 and S194-IgG1 was evaluated at 24 h, 48 h, and 72 h. (**B**) T Cytotoxicity mediated by S131-IgG1 and S194-IgG1 against PC-3, A549, and S15-A549 tumor cells was examined when the ratio between effector and target cells was 10:1. (**C**) Flow cytometry was performed to detect the relieving effect of S131-IgG1 and S194-IgG1 on the inhibition of the proliferation of human $CD3^+$T cells, $CD4^+$T cells, and $CD8^+$T cells mediated by the hsiglec-15 antigen (n≥3, ***P < 0.001and ****P < 0.0001, as determined by non-parametric test).

the volume of tumor cells in the group treated with S131-IgG1 was significantly reduced (Figure 6B), showing that S131-IgG1 inhibited tumor growth. In addition, the fluorescence intensity of tumor cells was significantly weakened after S131-IgG1 treatment (Figure 6C), which indicated a decrease in the activity or number of tumor cells. The effectiveness of S131-IgG1 was further verified by the change in fluorescence intensity.

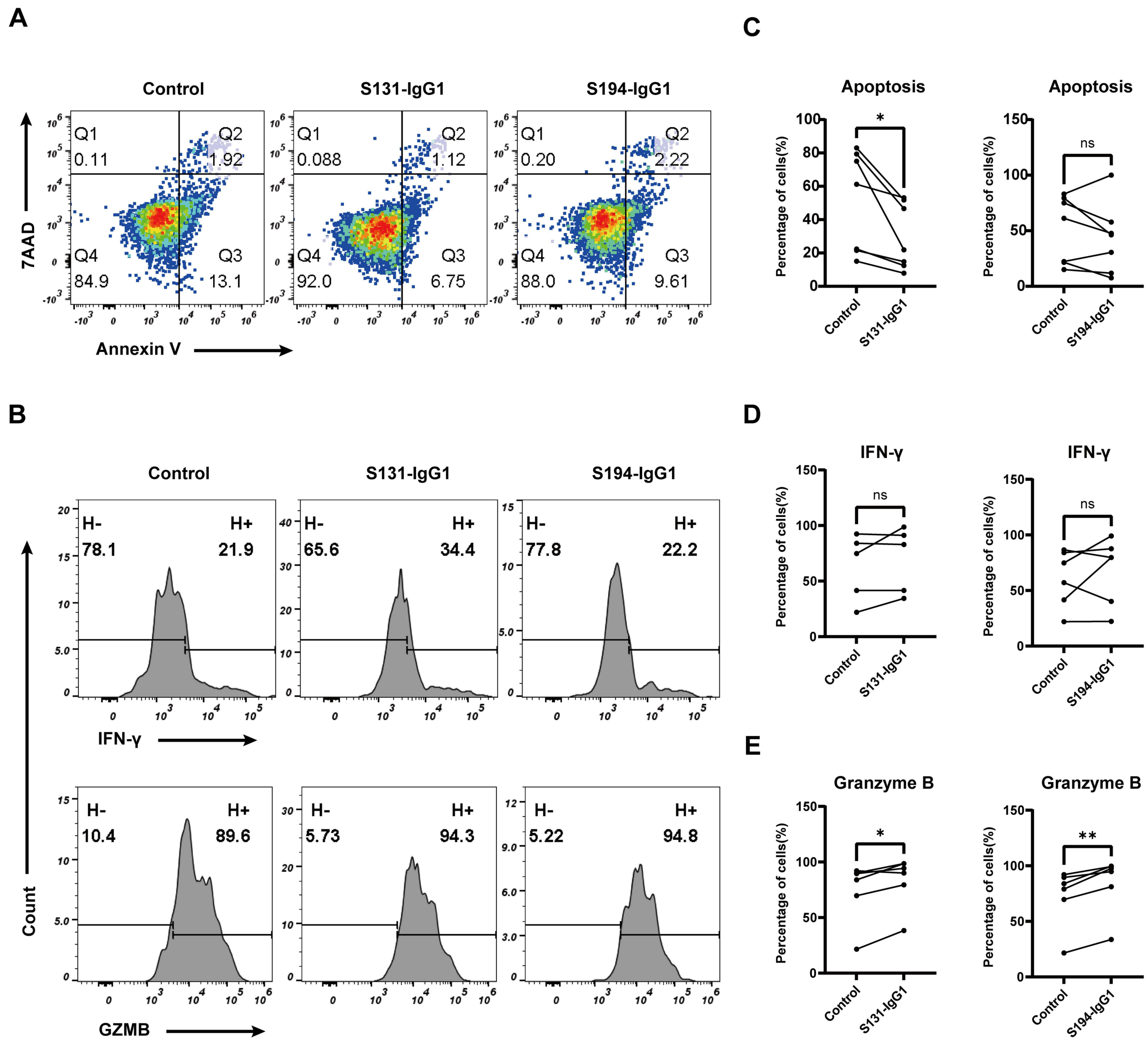

Figure 5 Antibody-Mediated Restoration of Exhausted CD8$^+$ T Cell Function. (**A**) Flow cytometry was performed to detect CD8$^+$ T cell apoptosis after S131-IgG1 and S194-IgG1 were co-cultured with PEMC. (**B**) The percentage of CD8$^+$ T cells apoptosis was determined. (**C**) Flow cytometry was performed to detect IFN-γ and GranzymeB produced by CD8$^+$ T cells after S131-IgG1 and S194-IgG1 were co-cultured with PEMC. (**D**) The percentage of IFN-γ produced by CD8$^+$ T cells was determined. (**E**) The percentage of CD8$^+$ T cells producing Granzyme B was evaluated (n≥6, ns indicates not statistically significant; *P < 0.05, **P < 0.01, as determined by paired *t*-tests).

Anti-siglec15 IgG1 Antibody Inhibited Tumor Growth and Promoted T-Cell Infiltration in a Humanized Mouse Tumor Model

The recombinant antibodies screened were fully human antibodies, therefore, we chose the PBMC humanized mouse tumor model as the in vivo mouse experimental model for antibody administration using the better functioning S131-IgG1 (Figure 7A). Mouse body weight was monitored throughout the treatment period (Figure 7B). Peripheral blood was collected, and tumor tissues were harvested and weighed, and the results showed that the tumor volume and weight of the mice in the control group were significantly increased (Figure 7C and D). Results from peripheral blood analysis in mice demonstrated that the proportion of hCD45$^+$ T cells exceeded 25%, indicating successful establishment of the humanized mouse model. Furthermore, no significant differences were observed in the proportions of hCD45$^+$, hCD3$^+$CD4$^+$, and hCD3$^+$CD8$^+$ T cells, suggesting consistent reconstitution levels across all experimental animals (Figure 7E), indicating that the recombinant antibody had a certain inhibitory effect on tumor growth in vivo. By detecting the proportion of

 https://doi.org/10.2147/ITT.S536009

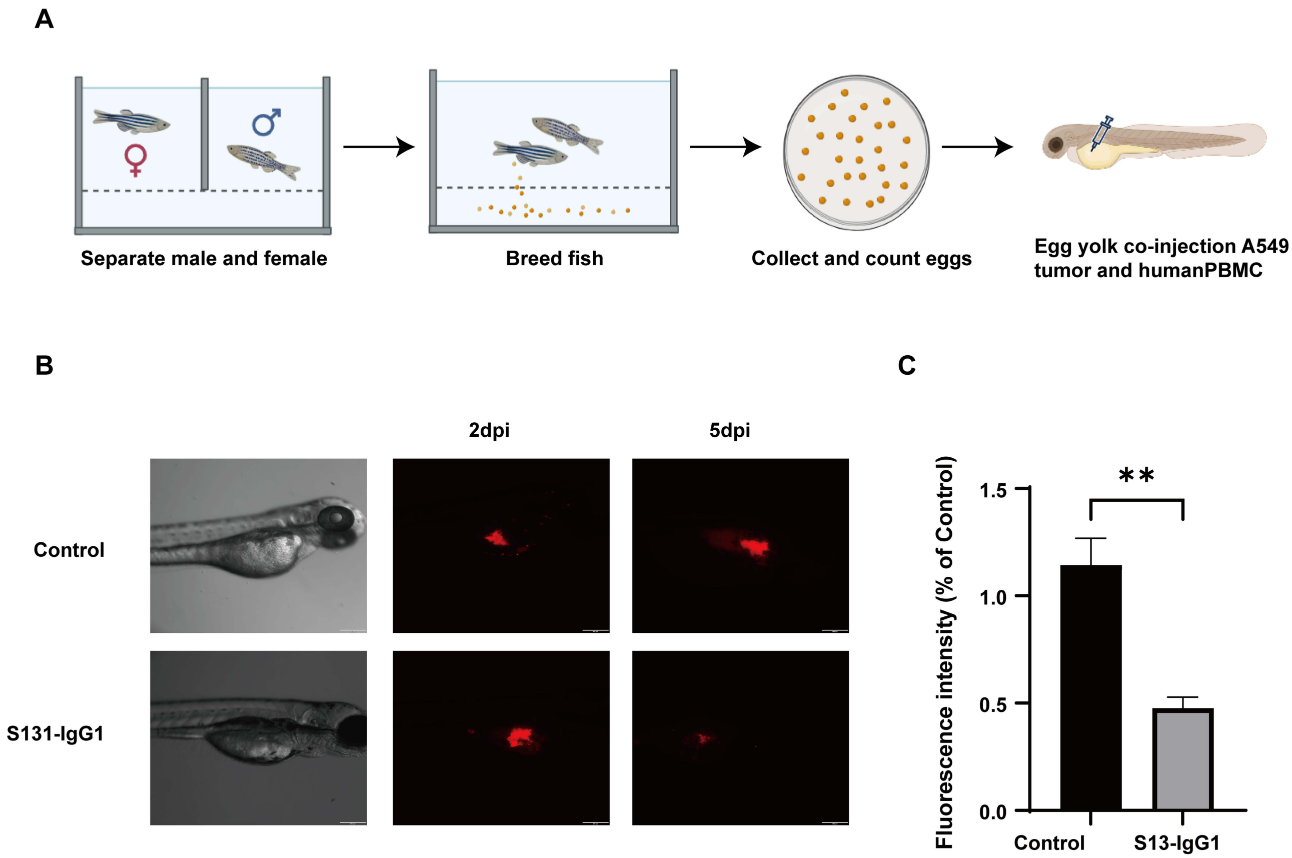

Figure 6 Antitumor Activity in Zebrafish Tumor Models. (**A**) Zebrafish model construction process. (**B**) Comparison of Dil-A549 tumor Fluorescence of zebrafish yolk sac in control and experimental groups. **(C)** Statistical analysis of zebrafish yolk sac tumor fluorescence intensity between control and experimental groups (n≥10, **P < 0.01, as determined by paired *t*-tests). dpi: days post-injection.

immune cells infiltrated in the tumor tissues of mice, we found that the infiltration of $HuCD45^+$ T cells in the tumor tissues of mice in the experimental group was significantly increased (Figure 7F). And the increase in the proportion of $HuCD45^+CD3^+$T cells indicated (Figure 7G) that T lymphocyte infiltration was mainly increased after antibody treatment, and $HuCD3^+CD8^+$T infiltration was predominant (Figure 7H). This reflects that the recombinant antibody has a good effect of targeting lymphocytes. In addition, $HuCD8^+CD69^+$ T and $HuCD4^+CD69^+$ T cells were also significantly increased (Figure 7I and J), indicating that the antibody inhibited tumor growth mainly by activating T lymphocytes infiltrating tumor tissues.

Discussion

High-affinity antibody drugs demonstrate therapeutic efficacy against refractory diseases including cancers and autoimmune disorders, phage display technology enables in vitro generation of these antibodies.[22] It has been found that the tumor microenvironment contains antibody-secreting cells (ASCs), which are associated with a favorable prognosis for several cancers, and patient-derived antibodies have diagnostic and therapeutic value.[23] High-affinity antibodies in cancer patients may inhibit tumor growth, especially those antibodies that act against antigens that are highly expressed in tumors. We established a high-diversity phage display library using lymph node samples from 20 lung cancer patients, successfully isolating siglec-15-specific scFvs subsequently converted to IgG1 antibodies. The candidate drug S194-IgG1 exhibited picomolar affinity (10^{-12} pmol), confirming the library's utility for discovering high-affinity antibodies. Furthermore, all antibodies specifically bound to human siglec-15 and showed no cross-reactivity with tumor antigens EphA2 or B7-H3. This target-specific binding capability, coupled with the ability to neutralize or enhance their activities, forms the foundation for therapeutic antibody development and engineering.[24]

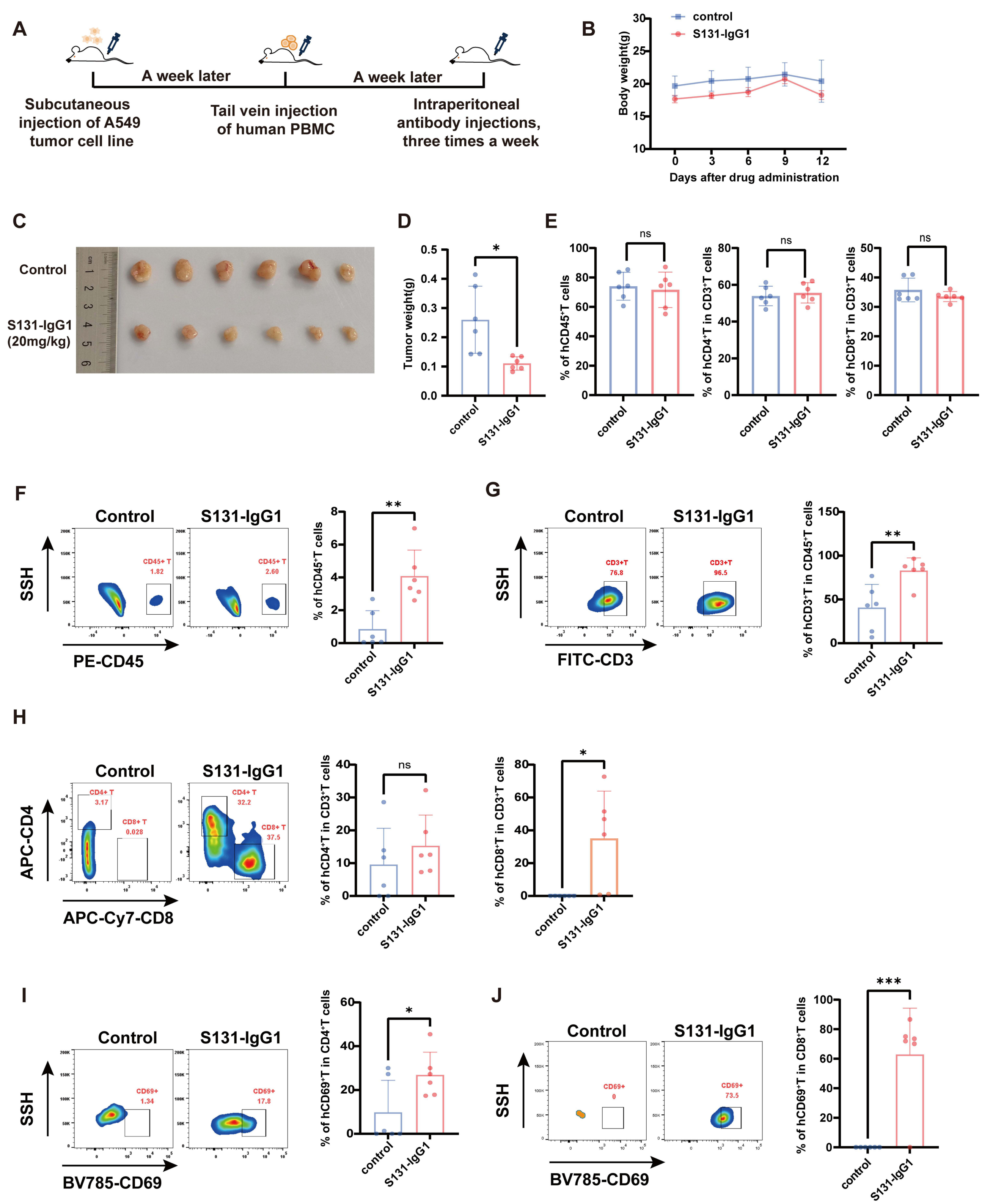

Figure 7 Tumor Suppression in Humanized Mouse Models. (**A**) The construction of the humanized mouse tumor model and the process of antibody administration are schematically represented. **(B)** Body weight change curves in mice post-dose. (**C**) Comparison of tumors between the control and experimental groups of mice. (**D**) Tumor weight of the mice in the control and experimental groups. (**E**) Proportions of hCD45$^+$, hCD3$^+$CD4$^+$, and hCD3$^+$CD8$^+$ T Cells in Mouse Peripheral Blood. (**F** and **G**) Flow cytometry was used to detect HuCD45$^+$T, HuCD45$^+$CD3$^+$T cells and their proportions in mouse tumor tissues. (**H**) Flow cytometry assays were performed to assess mouse tumor HuCD3$^+$CD4$^+$T cells, HuCD3$^+$CD8$^+$T cells, and their proportions. (**I** and **J**) Flow cytometry assays were performed to assess mouse tumor HuCD3$^+$CD4$^+$CD69$^+$T cells and HuCD3$^+$CD8$^+$CD69$^+$T cells proportions (n=6, ns indicates not statistically significant; *P < 0.05, **P < 0.01, and ***P < 0.001, as determined by unpaired *t*-tests).

This finding suggested that the anti-siglec15 IgG1 antibodies acted mainly by mediating ADCC and were associated with the expression of siglec-15. Studies have shown that when cytotoxic mechanisms such as ADCC and CDC are used to treat cancer, the ideal antigen should be confined to the tumor to minimize damage to healthy tissues.[25] Siglec-15 is lowly expressed in most normal tissues and immune cell subpopulations. However, it is widely upregulated in human cancer cells and M2-type macrophages in the tumor microenvironment, The limitation of siglec-15 expression contributes to the safety of recombinant antibody action.

Chen et al found that siglec-15 is a key immunosuppressive factor that is mutually exclusive with B7-H1 expression. It was also found that siglec-15 inhibits antigen-specific T cell responses primarily by regulating cell growth rather than apoptosis.[12] Using T-lymphocyte proliferation assays, we observed that the Siglec-15 antigen inhibited T-lymphocyte proliferation, consistent with findings by Chen et al. This inhibition was alleviated upon addition of anti-Siglec-15 IgG1 antibody, indicating partial blockade of Siglec-15 and reduced suppression of T-cell proliferation.

Malignant pleural effusion (MPE) represents a unique liquid tumor microenvironment (TME) where antitumor activity of innate (eg, NK cells) and adaptive (eg, CD8+ T cells) immune pathways is suppressed.[26,27] Zhao et al developed cyclic dinucleotide-loaded liposomal nanoparticles (LNP-CDN). In human MPE experiments, they observed CD8+ T cell generation, increased stem-like memory CD8+ T cells, and significant transcriptomic alterations in macrophage aggregates.[28] However, functional restoration of exhausted CD8+ T cells remains unexplored. Therefore, we re-stimulated lymphocytes from clinical MPE samples and observed reduced CD8+ T cell apoptosis alongside significantly increased granzyme B (GZMB) following anti-Siglec-15 IgG1 antibody treatment.

Additionally, Xiao et al developed a chimeric anti-Siglec-15 monoclonal antibody (S15-4E6A), demonstrating that anti-Siglec-15 IgG1 inhibits lung adenocarcinoma cell and xenograft tumor growth in vitro and in vivo by promoting M1 while suppressing M2 macrophage polarization[29]. However, effects on T lymphocyte activation and infiltration were not investigated. In our study, flow cytometry revealed increased human lymphocyte infiltration within treated murine tumor tissues. This anti-tumor effect was primarily mediated by CD8+ T cell infiltration and activation, suggesting anti-Siglec-15 IgG1 may offer an effective therapeutic strategy for lung cancer.

Although this study demonstrates the standalone therapeutic efficacy of anti-siglec-15 antibodies, the differential expression patterns of siglec-15 and PD-L1 in lung adenocarcinoma and their potential synergy remain unexplored. Given their mutually exclusive expression in human cancers, comparative analysis is crucial for validating siglec-15-targeted therapy as an alternative for PD-L1-insensitive tumors. Consequently, future work will compare siglec-15 antibodies with PD-1/PD-L1 inhibitors in PD-L1-insensitive models and evaluate combination efficacy. We will analyze murine tumor tissues using single-cell RNA sequencing (scRNA-seq) to identify CD8+ T cell-associated genes and pathways, elucidating mechanisms underlying antibody-mediated therapies.

Conclusion

We evaluated the feasibility of screening for siglec-15-targeting antibodies from a library derived from tumor patients. The affinity and specificity of the identified recombinant antibodies were determined, and their biological functions were analyzed. Research on siglec-15-targeting antibodies is highly significant for evaluating the normalization of immunotherapy within the tumor immune microenvironment, improving tumor treatment strategies, and enhancing therapeutic efficacy.

Abbreviations

ADCC, Antibody-dependent cellular cytotoxicity; TME, Tumor microenvironment; PD-L1, Programmed death ligand 1; EGFR, Epidermal growth factor receptor; NSCLC, Non small cell lung cancer; BLCA B, Ladder urothelial carcinoma; ASCs, Antibody-secreting cells; DMEM, Dulbecco's modified eagle medium; FBS, Fetal bovine serum; TMB, Tetramethylbenzidine; BLI, Bio-layer interferometry; PBMC, Peripheral blood mononuclear cell; SPF, Specific pathogen-free; SOE-PCR, Overlapping extension PCR; PEMC, Pleural effusion mononuclear cells; MPE, Malignant pleural effusion; scRNA-seq, Single-cell RNA sequencing.

Data Sharing Statement

The datasets generated and/or analyzed during the current study are available from the corresponding author upon reasonable request.

Ethics Approval and Consent to Participate

This study complied with the provisions of the Declaration of Helsinki. Ethical approval was obtained for all research involving human or animal subjects, and informed consent was secured from all human participants. Approval for human research was granted by the Experimental Ethics Committee of the Affiliated Hospital of Southwest Medical University (KY2023277), and for animal research by the Animal Experiment Ethics Committee of Southwest Medical University (20220812-030).

Acknowledgments

I would like to thank my supervisor, Prof. Yuan Qing, for her great support to my project. Thanks to her guidance and help, I was able to complete all my work. I would also like to thank Ms. Li Lin for her cooperation and help during the data collection process of my research project.

Author Contributions

All authors made a significant contribution to the work reported, whether that is in the conception, study design, execution, acquisition of data, analysis and interpretation, or in all these areas; took part in drafting, revising or critically reviewing the article; gave final approval of the version to be published; have agreed on the journal to which the article has been submitted; and agree to be accountable for all aspects of the work.

Funding

This work was supported by Sichuan Science and Technology Program (2025ZNSFSC0659); Luzhou Science and Technology Program (2023SYF100, 2024SYF128), The Science and Technology Strategic Cooperation Programs of Luzhou Municipal People 's Government and Southwest Medical University (2023LZXNYDJ020; 2023LZXNYDJ029) and the project of Southwest Medical University (2024ZKY037).

Disclosure

The authors declare that the submitted work was not carried out in the presence of any personal, professional, or financial relationships that could potentially be constructed as a conflict of interest.

References

1. Pan C, Liu H, Robins E, et al. Next-generation immuno-oncology agents: current momentum shifts in cancer immunotherapy. *J Hematol Oncol*. 2020;13(1):29.
2. Atkins MB, Lotze MT, Dutcher JP, et al. High-dose recombinant interleukin 2 therapy for patients with metastatic melanoma: analysis of 270 patients treated between 1985 and 1993. *J Clin Oncol*. 1999;17(7):2105–2116. doi:10.1200/JCO.1999.17.7.2105
3. Brudno JN, Kochenderfer JN. Toxicities of chimeric antigen receptor T cells: recognition and management. *Blood*. 2016;127(26):3321–3330.
4. O'Rourke K. ASCO releases guideline on CAR T-cell therapy: a multidisciplinary team's recommendations help in the recognition, workup, evaluation, and management of the most common chimeric antigen receptor (CAR) T-cell-related toxicities: a multidisciplinary team's recommendations help in the recognition, workup, evaluation, and management of the most common chimeric antigen receptor (CAR) T-cell-related toxicities. *Cancer*. 2022;128(3):429–430.
5. Sanmamed MF, Chen L. A paradigm shift in cancer immunotherapy: from enhancement to normalization. *Cell*. 2018;175(2):313–326. doi:10.1016/j.cell.2018.09.035
6. Sznol M, Chen L. Antagonist antibodies to PD-1 and B7-H1 (PD-L1) in the treatment of advanced human cancer--response. *Clin Cancer Res*. 2013;19(19):5542. doi:10.1158/1078-0432.CCR-13-2234
7. Taube JM, Anders RA, Young GD, et al. Colocalization of inflammatory response with B7-h1 expression in human melanocytic lesions supports an adaptive resistance mechanism of immune escape. *Sci Transl Med*. 2012;4(127):127ra137. doi:10.1126/scitranslmed.3003689
8. Zhang Y, Chen L. Classification of advanced human cancers based on Tumor Immunity in the MicroEnvironment (TIME) for cancer immunotherapy. *JAMA Oncol*. 2016;2(11):1403–1404. doi:10.1001/jamaoncol.2016.2450
9. Mittal D, Gubin MM, Schreiber RD, Smyth MJ. New insights into cancer immunoediting and its three component phases--elimination, equilibrium and escape. *Curr Opin Immunol*. 2014;27:16–25. doi:10.1016/j.coi.2014.01.004
10. Gajewski TF, Schreiber H, Fu Y-X. Innate and adaptive immune cells in the tumor microenvironment. *Nat Immunol*. 2013;14(10):1014–1022. doi:10.1038/ni.2703

11. Rashid S, Song D, Yuan J, Mullin BH, Xu J. Molecular structure, expression, and the emerging role of Siglec-15 in skeletal biology and cancer. *J Cell Physiol*. 2022;237(3):1711–1719. doi:10.1002/jcp.30654
12. Wang J, Sun J, Liu LN, et al. Siglec-15 as an immune suppressor and potential target for normalization cancer immunotherapy. *Nat Med*. 2019;25 (4):656–666. doi:10.1038/s41591-019-0374-x
13. Li B, Zhang B, Wang X, et al. Expression signature, prognosis value, and immune characteristics of Siglec-15 identified by pan-cancer analysis. *Oncoimmunology*. 2020;9(1):1807291. doi:10.1080/2162402X.2020.1807291
14. Zhang H, Xie Y, Hu Z, et al. Integrative analysis of the expression of SIGLEC family members in lung adenocarcinoma via data mining. *Front Oncol*. 2021;11:608113. doi:10.3389/fonc.2021.608113
15. Toki M, Zugazagoitia J, Altan M, Liu L, Rimm D. Abstract 3151: quantitative measurement of Siglec-15 expression in non-small cell lung cancer and its association with PD-L1, B7-H4 and tumor infiltrating lymphocytes. Paper presented at: Proceedings: AACR Annual Meeting 2019; March 29-April 3; 2019; Atlanta, GA.
16. Hu J, Yu A, Othmane B, et al. Siglec15 shapes a non-inflamed tumor microenvironment and predicts the molecular subtype in bladder cancer. *Theranostics*. 2021;11:3089.
17. Alexander IS, Michael SG, Jason H, et al. 756 First-in-human, open-label, multicenter, phase 1 clinical study to evaluate safety, tolerability, pharmacokinetics and pharmacodynamics of anti Siglec-15 PYX-106 in subjects with advanced solid tumors. *J ImmunoTher Cancer*. 2023;11(Suppl 1).
18. Yang Y, Nian S, Li L, et al. Fully human recombinant antibodies against EphA2 from a multi-tumor patient immune library suitable for tumor-targeted therapy. *Bioengineered*. 2021;12(2):10379–10400. doi:10.1080/21655979.2021.1996807
19. Little M, Welschof M, Braunagel M, et al. Generation of a large complex antibody library from multiple donors. *J Immunol Methods*. 1999;231 (1–2):3–9. doi:10.1016/S0022-1759(99)00164-7
20. Frenzel A, Kügler J, Wilke S, Schirrmann T, Hust M. Construction of human antibody gene libraries and selection of antibodies by phage display. *Methods Mol Biol*. 2014;1060:215–243.
21. Yin Z, Mao Y, Zhang N, et al. A fully chimeric IgG antibody for ROR1 suppresses ovarian cancer growth in vitro and in vivo. *Biomed Pharmacother*. 2019;119:109420. doi:10.1016/j.biopha.2019.109420
22. Nagano K, Tsutsumi Y. Phage display technology as a powerful platform for antibody drug discovery. *Viruses*. 2021;13(2):178. doi:10.3390/v13020178
23. Mazor RD, Nathan N, Gilboa A, et al. Tumor-reactive antibodies evolve from non-binding and autoreactive precursors. *Cell*. 2022;185(7):1208–1222.e21. doi:10.1016/j.cell.2022.02.012
24. Shim H. Bispecific antibodies and antibody-drug conjugates for cancer therapy: technological considerations. *Biomolecules*. 2020;10(3):360.
25. Goulet DR, Atkins WM. Considerations for the design of antibody-based therapeutics. *J Pharm Sci*. 2020;109(1):74–103. doi:10.1016/j.xphs.2019.05.031
26. Murthy P, Ekeke CN, Russell KL, et al. Making cold malignant pleural effusions hot: driving novel immunotherapies. *Oncoimmunology*. 2019;8(4):e1554969. doi:10.1080/2162402X.2018.1554969
27. Wang Z-H, Zhang P, Peng W-B, et al. Altered phenotypic and metabolic characteristics of FOXP3+CD3+CD56+ natural killer T (NKT)-like cells in human malignant pleural effusion. *Oncoimmunology*. 2023;12(1):2160558. doi:10.1080/2162402X.2022.2160558
28. Liu Y, Wang L, Song Q, et al. Intrapleural nano-immunotherapy promotes innate and adaptive immune responses to enhance anti-PD-L1 therapy for malignant pleural effusion. *Nat Nanotechnol*. 2022;17(2):206–216.
29. Xiao X, Peng Y, Wang Z, et al. A novel immune checkpoint siglec-15 antibody inhibits LUAD by modulating mφ polarization in TME. *Pharmacol Res*. 2022;181:106269. doi:10.1016/j.phrs.2022.106269